

Cite this: DOI: 10.1039/c0xx00000x

www.rsc.org/xxxxxx

PAPER

## Rapid electrochemical detection on a mobile phone

Peter B. Lillehoj<sup>a</sup>, Ming-Chun Huang<sup>b</sup>, Newton Truong<sup>c</sup> and Chih-Ming Ho<sup>d</sup>

Received (in XXX, XXX) Xth XXXXXXXXX 2013, Accepted Xth XXXXXXXXX 2013

DOI: 10.1039/b000000x

We present a compact mobile phone platform for rapid, quantitative biomolecular detection. This system consists of an embedded circuit for signal processing and data analysis, and disposable microfluidic chips for fluidic handling and biosensing. Capillary flow is employed for sample loading, processing, and pumping to enhance operational portability and simplicity. Graphical step-by-step instructions displayed on the phone assists the operator through the detection process. After the completion of each measurement, the results are displayed on the screen for immediate assessment and the data is automatically saved to the phone's memory for future analysis and transmission. Validation of this device was carried out by detecting *Plasmodium falciparum* histidine-rich protein 2 (PfHRP2), an important biomarker for malaria, with a lower limit of detection of 16 ng/mL in human serum. The simple detection process can be carried out with two loading steps and takes 15 min to complete each measurement. Due to its compact size and high performance, this device offers immense potential as a widely accessible, point-of-care diagnostic platform, especially in remote and rural areas. In addition to its impact on global healthcare, this technology is relevant to other important applications including food safety, environmental monitoring and biosecurity.

### Introduction

One of the greatest challenges in global healthcare is the lack of adequate diagnostic testing for early disease detection.<sup>1</sup> Conventional biomolecular assays, such as enzyme-linked immunosorbent assay (ELISA), Western blot, and lateral flow, generally require expensive facilities, costly equipment, and trained technicians which are not practical in most of the world, especially in developing countries. Microfluidics allows for substantial reductions in device size and costs while offering enhanced precision and automation.<sup>2-4</sup> This technology has facilitated the

development of integrated microsystems (lab-on-chips) that provide new diagnostic capabilities for addressing global health priorities.<sup>5,6</sup> However, these systems still require cumbersome components (pumps, sample processors, optical/electrical detectors) and complex setups for operation.<sup>7</sup> Recently, the concept of using mobile phones for improving healthcare, particularly in developing countries, has been proposed due to their ubiquitous availability.<sup>8,9</sup> As of 2012, there were 6 billion mobile phone subscribers worldwide (86% of the world's population) with most growth occurring in the developing world.<sup>10</sup> Additionally, the smartphone market is expected to grow by 50% by 2015, with new annual shipments approaching 1 billion units.<sup>11</sup> Mobile phones are also equipped with most of the components (i.e. processor, visual display, battery) required for a biodetector. Therefore, utilizing mobile phones for biomedical applications offers a unique approach to increase the availability and accessibility of diagnostic testing, especially in developing countries that lack adequate resources

<sup>a</sup> Department of Mechanical Engineering, Michigan State University, E. Lansing, MI, U.S.A. Tel: 517-432-2976; Email: lillehoj@egr.msu.edu.

<sup>b</sup> Computer Science Department, University of California, Los Angeles, CA, U.S.A.

<sup>c</sup> Electrical Engineering Department, University of California, Los Angeles, CA, U.S.A.

<sup>d</sup> Mechanical and Aerospace Engineering Department, University of California, Los Angeles, CA, U.S.A

and laboratory facilities. Towards this end, mobile phone-based oximeters have been developed for measuring oxygen content in blood.<sup>12,13</sup> Recent studies have also demonstrated microscopy using mobile phones applicable to disease diagnosis and water quality monitoring.<sup>14-17</sup> These systems integrate a compact imaging device with a phone's CCD camera for detecting microorganisms as a means for biodetection and diagnosis.<sup>18,19</sup> However, the applicability of these devices for detecting protein/nucleic acid disease biomarkers is limited. Many optical-based immunoassays only provide qualitative ("positive" or "negative") or visual readouts which can be ambiguous and difficult to interpret. In contrast, quantitative biomarker measurements offer an accurate and reproducible means for disease prognosis, diagnosis and monitoring.<sup>20,21</sup> To accommodate these requirements, we have developed a mobile phone-based platform for quantitative biomolecular detection.

telecommunication capabilities. This system utilizes a highly sensitive electrochemical detection scheme that is capable of detecting a broad spectrum of biomolecules.<sup>22-24</sup> Amperometric measurements are carried out by an embedded circuit that plugs into the micro-USB port of the phone. Poly(dimethylsiloxane) (PDMS) microfluidic chips offer a disposable platform to process and analyze samples, which are driven by capillary flow for enhanced portability and improved automation. This greatly reduces the overall size of the device and eliminates the need for pumps or peripheral components. Through the integration and optimization of each module in our system, we have developed a device that is extremely transportable, easy-to-use, and capable of rapid measurements. To demonstrate the practicality of this system for diagnostic testing, we performed studies to assess the sensitivity and specificity for detecting the *Pf*HRP2 protein, a key clinical biomarker of the malaria parasite. Malaria is one of the most deadly infectious diseases worldwide, causing 655,000 deaths in 2010.<sup>25,26</sup> *Pf*HRP2 was detected in human serum at concentrations as low as 16 ng/mL. Each test can be carried out with 2 loading steps and completed within 15 min, thereby minimizing the time and complexity associated with diagnostic testing.

## Results and discussion

### Design of the microfluidic chip

Microfluidic chips are designed for simplified sample loading and autonomous liquid transport on miniaturized platforms. As shown in Fig. 1B, the entire chip measures 25 mm × 15 mm, which is the same size as a mobile phone subscriber identity module (SIM) card. This was achieved, in part, by utilizing a hydrophilic PDMS surface coating, which enables for capillary flow. Capillary-driven flows have the advantage of producing steady flow rates, which is primarily governed by the contact angle of the liquid with the channel walls and the channel geometry. Because these variables are fixed in our chip, there is minimal variation in the overall flow rate. There are two inlets and one outlet, which are 1 mm in diameter. The inlets are designated for loading of the sample and reporter solutions,

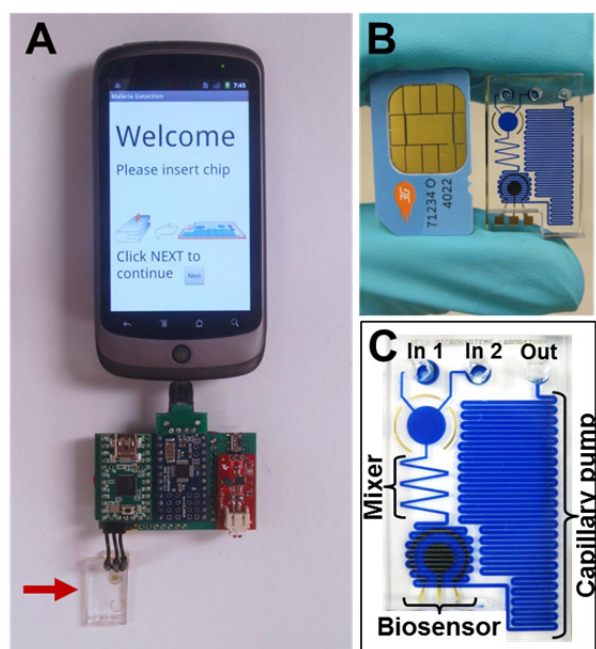


Figure 1. (A) Photograph of the assembled prototype device. The arrow indicates the microfluidic chip. (B) Photograph of the chip and a mobile phone SIM card for comparison. (C) An enlarged image of the chip with labeled components. The channels are filled with dye for improved visualization of the fluidic network.

A photograph of our device is shown in Fig. 1A. The smart phone functions as the chip reader and provides a simple user interface with

which can be loaded separately or simultaneously. Due to the hydrophilic nature of the channel walls, liquids are autonomously driven within the fluidic network. Sample loading is achieved simply by dispensing liquids into the chip inlets using a pipette or dropper. Downstream of the inlets is a 2 mm chamber which provides a region for the solutions to merge prior to entering a zig-zag mixer. Based on the channel geometry, we calculated the appropriate volumes of the sample (0.5  $\mu\text{L}$ ) and reporter (2.0  $\mu\text{L}$ ) solutions to synchronize their positions within the chip for subsequent fluidic processing. If the sample and reporter solutions are loaded simultaneously, they merge in the chamber at the same instant. If loaded separately, the sample is dispensed first. Due to its smaller volume, the sample only partially fills the chamber. When the larger volume of reporter solution is dispensed, it fills the remainder of the chamber and merges with the sample flow into the mixer. Following the mixer is a tightly-packed serpentine channel which is situated over an electrochemical sensor. From our volume calculation, the sample-reporter mixture stops flowing when this section is filled, leaving the remainder of the channel empty. Rather than encasing the sensor with a single chamber, we designed a serpentine channel which enables uniform passage of the sample-reporter mixture over the sensor surface. This not only improves protein recognition and overall detection sensitivity, but also provides sufficient surface contact area for PDMS-glass bonding. Fig. 1C provides a visual reference of the narrow spacing (40  $\mu\text{m}$ ) between the channels. The last stage of the chip is a secondary serpentine channel that functions as a capillary pump and serves as the waste reservoir. This section accommodates a 3,3',5,5'-tetramethylbenzidine/ hydrogen peroxide (TMB/ $\text{H}_2\text{O}_2$ ) substrate for washing and enzymatic reaction for subsequent amperometric measurements. The total effective length of this channel is 25 cm, which provides sufficient capacity for all the solutions loaded into the chip. All the channels are 400  $\mu\text{m}$  in width and 100  $\mu\text{m}$  in height, which allows for quick liquid transport where the entire chip is filled within a few min.

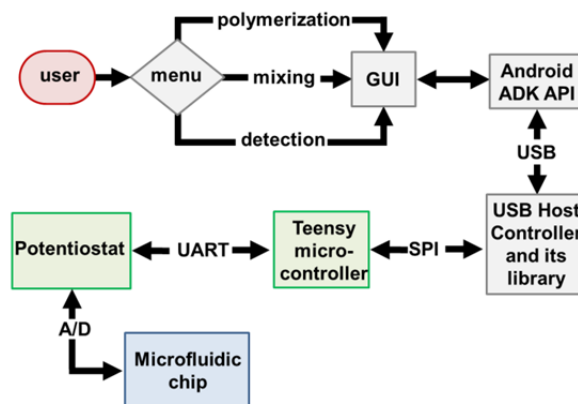


Figure 2. Flowchart depicting the user interaction with the Android interface. An electrical circuit enables data input from the user to the phone and data collection from the microfluidic chip to the phone.

### User interface and data communication

This platform provides a simplified user interface to guide the operator through the detection process. We have designed a customized Android application (app) to provide step-by-step instructions to facilitate user operation. A flowchart depicting the interaction between the user and our system is shown in Fig. 2. Upon insertion of the circuit into the phone, the Android operating system (OS) detects the USB insertion signal and triggers the app to initiate the detection cycle. A menu is displayed on the home screen allowing the user to select from a list of processes. Currently, this app supports three processes: electropolymerization, electric-field pulsed mixing, and amperometric detection. Once a process is selected, a second menu is displayed for adjusting parameters relevant to the process (e.g. applied voltage, duration). The recommended values for this assay are preset; however, this option is included to allow users to modify each program for other detection protocols. The app sends these parameters via USB connection, with the Android open accessory protocol, to the microcontroller. A preloaded USB host driver on the microcontroller accepts the USB connection and transmits the information accordingly. Once the communication is established between the phone and the microcontroller, it receives commands from user inputs and requests data from the potentiostat module. This module measures voltage and current signals from the

microfluidic chip and sends the data to the microcontroller using the universal asynchronous receiver/transmitter (UART) serial communication protocol. The microcontroller processes the received data packets by reassembling the messages and routes it back to the phone in real-time. Data visualization and analyses (denoising) is performed by the app on the phone.

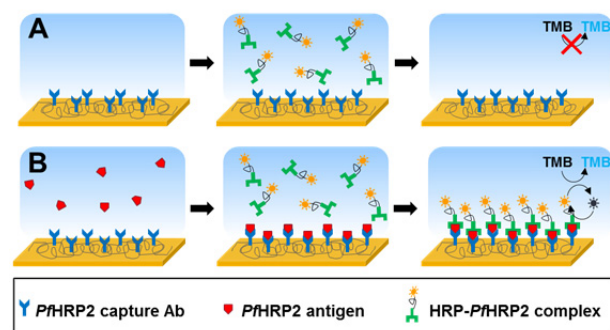


Figure 3. Illustration of the electrochemical detection scheme in the absence (A) and presence (B) of *PfHRP2* antigen.

#### *PfHRP2* detection

Detection of *PfHRP2* is achieved by combining a highly-specific protein binding scheme with high sensitivity enzymatic amplification. *PfHRP2* capture antibodies are immobilized on the electrode surface within a robust polypyrrole (PPy) matrix. The polymerization process results in a uniform surface coating having a thickness of  $27.5 \text{ nm} \pm 4.5 \text{ nm}$ . A reporter solution contains *PfHRP2* detection antibodies conjugated to horseradish peroxidase (Px) in Dulbecco's phosphate-buffered saline (DPBS). In the absence of *PfHRP2* antigen, the detection antibodies are unable to bind to the surface and are subsequently washed away when the TMB/ $\text{H}_2\text{O}_2$  substrate is loaded into the chip (Fig. 3A). When a voltage potential is applied, a negligible electrochemical current is generated, which is caused by spontaneous oxidation of the TMB substrate over time. In the presence of *PfHRP2* antigen, the detection antibodies bind to the sensor surface through the antigen (Fig. 3B). Application of the TMB/ $\text{H}_2\text{O}_2$  substrate with a voltage potential results in a substantial electrochemical current directly proportional to the concentration of *PfHRP2* protein in the sample.

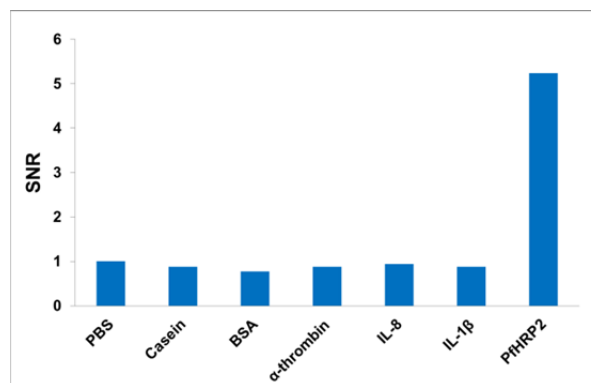


Figure 4. Specificity of *PfHRP2* antigen binding to *PfHRP2* capture antibody. Measurements were performed using *PfHRP2* antigen, IL-1 $\beta$ , IL-8,  $\alpha$ -thrombin and BSA diluted in PBS at concentrations of  $1 \text{ } \mu\text{g/mL}$ , 0.1% casein in DPBS and DPBS (blank). Each bar represents the average value over three separate measurements.

The specificity of the sensor was determined using a purified *PfHRP2* recombinant protein and 5 irrelevant target proteins in DPBS. At  $1.0 \text{ } \mu\text{g/mL}$ , the *PfHRP2* antigen produced a signal-to-noise ratio (SNR) of 5.3 (Fig. 4). By contrast, all of the irrelevant proteins at the same concentration generated a SNR equal to that of the DPBS blank control. To assess the sensitivity of the sensor, human serum was spiked with increasing concentrations of *PfHRP2* ( $4$ – $1,024 \text{ ng/mL}$ ). As shown in Fig. 5A, amperometric signals at all concentrations were clearly distinguishable above unspiked serum ( $0 \text{ ng/mL}$ ). All signals exhibited relatively smooth response profiles with minimal noise. Measurements are taken over 60 sec, with the final 15 sec averaged to generate the dose-response profile with a lower limit of detection (LOD) of  $16 \text{ ng/mL}$  (Fig. 5B). This LOD is similar to that reported for many clinically relevant disease biomarkers<sup>27</sup> including other *PfHRP2* amperometric immunosensors.<sup>28,29</sup> Further optimization of the assay system will improve detection sensitivity. For example, a faster flow rate may enhance washing of the reporter solution from the sensor and result in a lower background signal. Also, the sensitivity of the sensor could be enhanced by employing conductive nanoparticles to facilitate signal transduction.



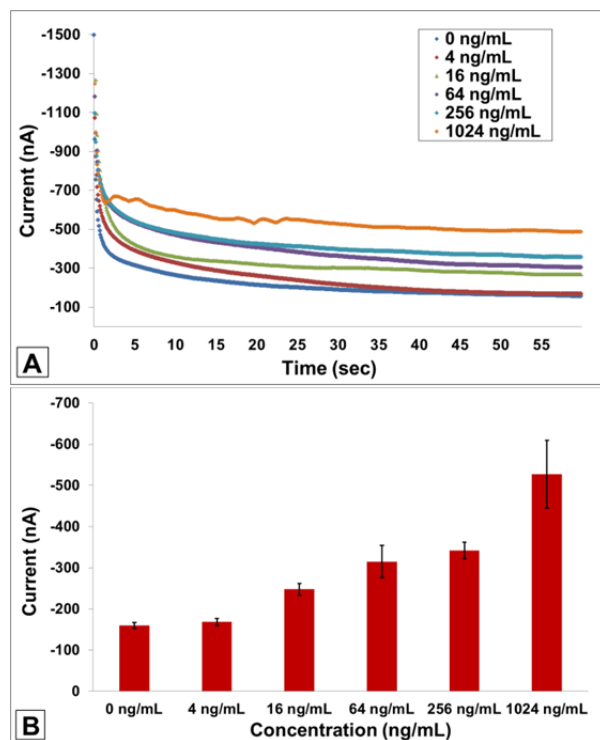


Figure 5. Electrochemical detection of *PfHRP2* antigen in human serum. (A) Representative amperometric measurements of increasing *PfHRP2* antigen concentrations at -200 mV. (B) Concentration profile for *PfHRP2* antigen detection. Values are averaged over the final 15 sec of amperometric measurements. Each bar represents the mean  $\pm$  standard deviation of three separate measurements.

## Materials and methods

### Fabrication materials

Silicon and glass wafers (100 mm diameter, 500  $\mu$ m thickness) were obtained from TechGophers Corp. (Los Angeles, CA). PDMS prepolymer and curing agents (Sylgard 184) were obtained from Dow Corning (Midland, MI). PEG (MW 200) was obtained from Sigma-Aldrich (St. Louis, MO). Colored dye for flow visualization was purchased from a local vendor. KMPR 1050 was obtained from MicroChem Corp. (Newton, MA). AZ 4620 photoresist (Shipley, Marlborough, MA), hexamethyldisilazane (HDMS), acetone, isopropanol and methanol were obtained from the UCLA Nanoelectronics Research Facility

### Fabrication of the microfluidic chips

The fabrication of microfluidic chips follows closely with previously reported PDMS devices.<sup>30</sup> Gold electrodes were fabricated on glass substrates and employed as electrochemical sensors. Metals were evaporated (CHA Mark 40) on a photolithographically-defined AZ4620 photoresist shadow mask. Cr and Au were sequentially deposited with thicknesses of 20 nm and 200 nm respectively. Lift off was performed via sonication in acetone followed by rinsing in deionized (DI) water. Individual chips were cut using a glass cutter. PDMS molds were fabricated by photolithography of KMPR 1050 photoresist on Si wafers. PDMS prepolymer and curing agents were mixed, degassed and poured onto the molds, and cured for 2 hr at 80°C. Individual chips were cut and inlet/outlet holes were punched. A hydrophilic surface treatment was performed on the PDMS chips to facilitate capillary pumping.<sup>31</sup> Briefly, PDMS surfaces were exposed to an air plasma (Harrick, Ithaca, NY) for 90 sec. PEG was immediately dispensed onto the oxidized surfaces and the chips were heated to 150°C for 25 min. Once cooled, the chips were rinsed in isopropanol and DI water and dried using purified N<sub>2</sub>. Following surface treatment, PDMS channels were assembled together with glass chips.

### Assay chemicals and reagents

*PfHRP2* antibodies and recombinant *PfHRP2* antigen were from CTK Biotech, Inc. (San Diego, CA). IL-1 $\beta$  and IL-8 recombinant proteins were from Sigma-Aldrich (St. Louis, MO). Human  $\alpha$ -thrombin was from Haematologic Technologies, Inc. (Essex Junction, VT). Human serum was from Bioreclamation, LLC (Hicksville, NY). Bovine serum albumin (BSA), 0.1% casein in PBS and DPBS were from Thermo Scientific (Tustin, CA). Polypyrrole (PPy) and KCl were from Sigma. TMB/H<sub>2</sub>O<sub>2</sub> was from Neogen (Lexington, KY). DI water (18.3 M $\Omega$ -cm) was generated using a Barnstead Easypure II water purification system.

### Electrical components

USB host shields were from Circuits@Home. Teensy 2.0 microcontrollers and 3.3 voltage

regulators (part no. MCP1825) were from PJRC.com, LLC. (Sherwood, OR). LiPower power controllers (part no. PRT-10255), logic level shifters (part no. BOB-08745) and polymer lithium ion batteries (part no. PRT-00339) were from SparkFun Electronics (Boulder, CO). Potentiostat circuits were from Palm Instruments BV (Houten, Netherlands). Miscellaneous components (capacitors, resistors, contact pins, wires) were from Digi-Key (Thief River Falls, MN).

### Design and assembly of the circuit

An electrical circuit was developed to provide an interface between the microfluidic chip and the mobile phone. The main functions of this circuit are to interpret the commands that the user inputs into the phone, send required parameters for the electrochemical measurements, and receive the detected signal from the sensor back to the mobile phone. To automate all of these operations, this circuit employs a USB host shield, a programmable microcontroller, a potentiostat, a logic level shifter, a voltage regulator and a battery. A custom printed circuit board (PCB) was designed using Altium Designer and fabricated by Sunstone Circuits (Mulino, OR) to integrate all of the components for electrical communication and power distribution. A schematic of the PCB connection layout is shown in Fig. 6. The overall dimensions of the PCB are 35 mm by 57 mm. The connection points have a pitch of 0.1 in, which allows for adequate spacing and flexible placement of the traces. A 5 V trace, which provides power to the PCB, was designed to be 0.115 in wide, enabling for the transmission of larger currents. An unoccupied region on the top layer of the board is filled with copper and electrically grounded. The unoccupied region on the bottom layer is also filled with copper but is electrically connected to 3.3 V. Most of the components in this circuit require 3.3 V to operate and this is an effective method to distribute the power. The diameters of the header pins and through holes are 0.025 in and 0.055 in respectively, which allows for ample spacing for component adjustment and fitting. Each component is individually soldered through the header pins to ensure a rigid connection.

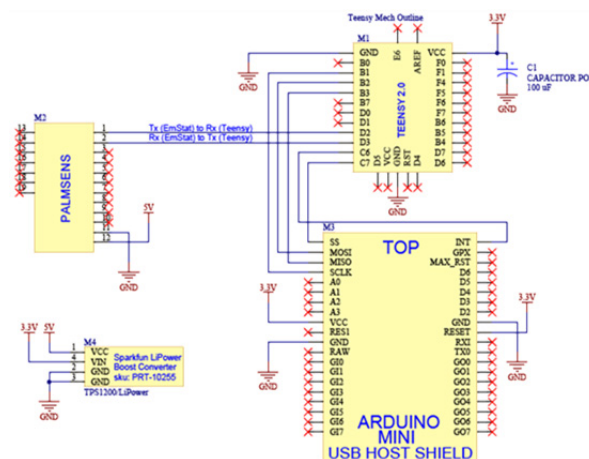


Figure 6. Schematic illustration of the PCB layout depicting the electrical connections between the various components.

In this prototype, we used a Nexus One mobile phone running on the Android 2.3.4 operating system (OS). Ideally, any mobile phone with a USB connector should link with a USB-equipped accessory. However, this is only valid if the phone can operate as a USB host device during initial USB recognition. Mobile phones running on older versions of Android that do not support USB host functionality cannot be exploited to communicate with USB-equipped accessories. Therefore, to make our device backwards compatible with phones running on USB client mode-only versions of Android, we employed a microcontroller and USB host shield to operate as a USB host-enabled accessory powered by a lithium ion battery. By doing so, any Android phone with a micro-USB port and Android open accessory protocol can be used with our circuit. In order to allow the microcontroller to support USB host mode, a **USB host shield** was employed to provide USB connectivity and USB packet reassembling. To function as a USB host mode accessory, a 5 V voltage is required to initiate USB communication provided by the host device. Most low-cost rechargeable batteries only provide ~3.7 V; therefore, we designed a circuit to include a voltage regulator to boost voltages from 3.7 V to 5 V in order to provide the bootstrap voltage for completing USB initialization. **The side effect of boosting the voltage is that the digital transmission voltage shifts accordingly.** To address this issue, we employed a **logic level shifter** to convert the digitalized signal of the microcontroller to a

corresponding voltage level to maintain communication between the USB host shield to the microcontroller and the microcontroller to the potentiostat. We developed custom firmware which consists of USB, serial and simulated serial communication libraries to integrate all components together. This firmware is preloaded in the non-volatile ROM of the microcontroller and is designed to initiate immediately when the power is provided to the circuit.

### Electrode surface modification

The sensor surface was modified by forming a conductive PPy layer, facilitating protein immobilization and enhancing detection sensitivity. This method of antibody immobilization results in excellent long-term stability where no significant loss in protein activity is observed for up to one year.<sup>32</sup> For this reason, we envision that this process can be performed prior to packaging the chips. The PPy layer was generated through electropolymerization of a polymer solution consisting of *Pf*HRP2 capture antibodies (10 µg/mL) diluted in DPBS containing 0.2 M KCl and polypyrrole (1:150). Electropolymerization was carried out by dispensing 20 µL of polymer solution onto the sensor and applying a square-wave electrical field consisting of 9 sec at +350 mV and 1 sec at +950 mV. The entire process consisted of 20 cycles, followed by rinsing in ultrapure DI water and drying with compressed N<sub>2</sub>. The thickness of the coating was determined using a Dektak 6 profilometer.

### Electrochemical detection procedures

All electrochemical measurements were performed using the mobile phone platform. Prior to sample loading, the circuit was connected to the phone and a new microfluidic chip was inserted into the device. 0.5 µL of *Pf*HRP2 antigen at varying concentrations was dispensed into inlet 1 and 2.0 µL of reporter solution was dispensed into inlet 2 of the chip. For assay selectivity measurements, target proteins were diluted to 1.0 µg/mL in DPBS. The concentration profile was obtained by diluting *Pf*HRP2 antigen in human serum. By capillary flow, the two solutions were driven through the channels and mixed upon passage through the zig-zag mixer. After the solution

filled the channels over the sensor, a square-wave electrical field, consisting of 20 cycles of 9 sec at -300 mV and 1 sec at +200 mV, was applied to the sensor via the phone app. This pulsed field allows for improved protein recognition and binding to the electrode surface. 7.0 µL of TMB/H<sub>2</sub>O<sub>2</sub> substrate was dispensed into inlet 1, followed by amperometric measurements at -200 mV for 60 sec. Sample loading was carried out using a pipette and subsequent fluidic transportation was driven by capillary flow. Blank control measurements (without *Pf*HRP2 antigen) were performed using new chips and all measurements were performed at room temperature.

### Conclusions

We present a mobile phone platform for biomolecular analytical detection. This device utilizes a compact circuit for rapid, high sensitivity electrochemical measurements. Sample handling, pumping and sensing is carried out on disposable microfluidic chips employing capillary flow for power-free fluidic operation. We detected *P. falciparum* HRP2 antigen in human serum at 16 ng/mL. This assay demonstrates high specificity with *Pf*HRP2 proteins exhibiting a SNR 5-fold greater than those of irrelevant proteins. This system offers a simplified user interface, providing graphical, step-by-step instructions through a custom Android app. In contrast to commercial lateral flow immunoassays that only provide a positive/negative readout,<sup>33,34</sup> this platform provides quantifiable measurements directly proportional to biomarker concentration. In contrast to commercial ELISAs that require 2-3 hr analysis times, this mobile phone-based assay is completed in 15 min and can be carried out with 2 loading steps (if the sample and reporter solutions are loaded simultaneously). In the immediate application of this device, rapid and sensitive *Pf*HRP2 quantification permits an accurate diagnosis of individuals with reoccurring malaria infection.<sup>35</sup> For future applications, we plan to perform field testing and implement wireless data transmission functionality. Ultimately, this device offers an innovative means for rapid, high sensitivity, quantitative measurements on a fully handheld platform, and has the potential to greatly improve the availability and accessibility of

diagnostic testing worldwide, especially in remote rural areas.

## Acknowledgements

The work was supported by the Bill and Melinda Gates Foundation (GCGH # 442561-HC-80086). We thank Joel Wong for his help in various aspects of the project, Dr. Vincent Gau for advice on electrochemical detection, Dr. Fang Wei for advice on assay optimization and Jessica Wen for designing the graphics for the phone app.

## References

- 1 C. A. Petti, C. R. Polage, T. C. Quinn, A. R. Ronald and M. A. Sande, *Clin Infect Dis*, 2006, **42** (3), 377-382.
- 2 C. M. Ho and Y. C. Tai, *Annu Rev Fluid Mech*, 1998, **30**, 579-612.
- 3 D. C. Duffy, J. C. McDonald, O. J. A. Schueller and G. M. Whitesides, *Anal Chem*, 1998, **70**, 4974-4984.
- 4 M. A. Unger, H. Chou, T. Thorsen, A. Scherer, and S. R. Quake, *Science*, 2000, **288**, 113-116.
- 5 P. Yager, T. Edwards, E. Fu, K. Helton, K. Nelson, M. R. Tam and B. H. Weigl, *Nature*, 2006, **442**, 412-418.
- 6 C. D. Chin, V. Linder and S. K. Sia, *Lab Chip*, 2007, **7**, 41-57.
- 7 G. M. Whitesides, *Nature*, 2006, **442**, 368-373.
- 8 L. Bellina and E. Missoni, *Diagn Pathol*, 2009, **4** (19).
- 9 Grand Challenges in Global Health, Round 5 topics, 2010, <http://www.grandchallenges.org/MeasureHealthStatus/Topics/CellPhoneApps/Pages/Round5.aspx>
- 10 International Telecommunication Union, Statistics, 2012, [http://www.itu.int/ITU-D/ict/statistics/at\\_glance/KeyTelecom.html](http://www.itu.int/ITU-D/ict/statistics/at_glance/KeyTelecom.html)
- 11 International Data Corporation, Worldwide Quarterly Mobile Phone Tracker, 2011, <http://www.idc.com/getdoc.jsp?containerId=prUS22871611>
- 12 A. H. Khandoker, J. Black and M. Palaniswami, *Proceedings of the 6<sup>th</sup> ICECE 2010*, 634 – 637.
- 13 W. Karlen, G. Dumont, C. Peterson, J. Gow, J. Lim, J. Sleiman and J. M. Ansermino, *Proceedings of the ICHI 2011*, 433-438.
- 14 D. N. Breslauer, R. N. Maamari, N. A. Switz, W. A. Lam and D. A. Fletcher, *PLoS ONE*, 2009, **4** (7), e6320.
- 15 D. Tseng, O. Mudanyali, C. Oztoprak, S. O. Isikman, I. Sencan, O. Yaglidere and A. Ozcan, *Lab Chip*, 2010, **10**, 1787-1792.
- 16 Z. J. Smith, K. Chu, A. R. Espenson, M. Rahimzadeh, A. Gryshuk, M. Molinaro, D. M. Dwyre, S. Lane, D. Matthews and S. Wachsmann-Hogiu, *PLoS ONE*, 2011, **6** (3), e17150.
- 17 H. Zhu, O. Yaglidere, T.-W. Su, D. Tseng and A. Ozcan, *Lab Chip*, 2011, **11**, 315-322.
- 18 W. H. Wernsdorfer, in *Malaria: principles and practice of malariology*, ed. I. S. McGregor, Churchill Livingstone, 1988.
- 19 T. Hänscheid, C. M. Ribeiro, H. M. Shapiro and N. G. Perlmuter, *Lancet*, **7** (4) 236-237.
- 20 J. D. Wulfschuhle, C. P. Paweletz, P. S. Steeg, E. F. Petricoin III and L. Liotta, in *New Trends in Cancer for the 21<sup>st</sup> Century*, ed. A. Lombart-Bosch, J. A. Lopez-Guerrero and V. Felipo, Springer, 2003, vol. 532, pp. 59-68.
- 21 T. Pisitkun, R. Johnstone and M. A. Knepper, *Mol Cell Proteomics*, 2006, **5**, 1760-1771.
- 22 J. Wang, *Talanta*, 2002, **56** (2), 223-231.
- 23 F. Wei, P. B. Lillehoj and C. M. Ho, *Pediatr Res*, 2010, **67** (5), 458-468.
- 24 T. G. Drummond, M. G. Hill and J. K. Barton, *Nat Biotechnol*, 2003, **21** (10), 1191-1199.
- 25 World Health Organization, *World Malaria Report 2010*.
- 26 R. W. Snow, C. A. Guerra, A. M. Noor, H. Y. Myint and S. I. Hay, *Nature*, 2005, **434**, 214-217.
- 27 N. Rifai, M. A. Gillette and S. A. Carr, *Nat Biotechnol*, 2006, **24** (8), 971-983.
- 28 M. K. Sharma, V. K. Rao, G. S. Agarwal, G. P. Rai, N. Gopalan, S. Prakash, S. K. Sharma and R. Vijayaraghavan, *J Clin Microbiol*, 2008, **46** (11), 3759-3765.
- 29 M. K. Sharma, V. K. Rao, S. Merwyn, G. S. Agarwal, S. Upadhyah and R. Vijayaraghavan, *Talanta*, 2011, **85** (4), 1812-1817.
- 30 P. B. Lillehoj, F. Wei and C. M. Ho, *Lab Chip*, 2010, **10** (17), 2265-2270.
- 31 P. B. Lillehoj and C. M. Ho, Proceedings of the 23<sup>rd</sup> IEEE International Conference on Micro Electro Mechanical Systems (MEMS), Hong Kong, 2010.
- 32 S. Cosnier, *Anal Bioanal Chem*, 2003, **377**, 507-520.
- 33 A. Moody, *Clin Microbiol Rev*, 2002, **15** (1), 66-78.
- 34 C. K. Murray, R. A. Gasser Jr., A. J. Magill and R. S. Miller, *Clin Microbiol Rev*, 2008, **21** (1), 97-110.
- 35 I. C. E. Hendriksen, J. Mwanga-Amumpaire, L. von Seidlein, G. Mtove, L. J. White, R. Olaosebikan, S. J. Lee, A. K. Tshefu, C. Woodrow, B. Amos, C. Karema, S. Saiwaew, K. Maitland, E. Gomes, W. Pan-Ngum, S. Gesase, K. Silamut, H. Reyburn, S. Joseph, K. Chotivanich, C. I. Fanello, N. P. J. Day, N. J. White and A. M. Dondorp, *PLoS Med*, 2012, **9** (8), e1001297.